

Inclusion Complexes and Guest-Induced Color Changes of pH-Indicator-Modified  $\beta$ -Cyclodextrins

Tetsuo Kuwabara,\* Asao Nakamura, Akihiko Ueno,\* and Fujio Toda\*

Department of Bioengineering, Faculty of Bioscience and Biotechnology, Tokyo Institute of Technology, 4259 Nagatsuta-cho, Midori-ku, Yokohama 227, Japan

Received: April 21, 1994\*

A methyl red-modified  $\beta$ -cyclodextrin (**1**) and a *p*-methyl red-modified one (**2**), both being the structural isomers with a positional difference of one substituent in the appending dye part, were synthesized in order to attain color changes induced by host-guest complexation as well as to investigate their conformations and binding properties. The structures of **1** and **2** were investigated by UV-visible absorption and induced circular dichroism spectroscopy in a 10% ethylene glycol aqueous solution. Host **1** accommodates the methyl red moiety in its own  $\beta$ -CD cavity with an orientation parallel to the CD axis, forming an intramolecular complex, while **2** partially includes the *p*-methyl red moiety in its own  $\beta$ -CD cavity with an orientation perpendicular to the CD axis. In neutral media, both **1** and **2** exist as azo forms, which have the dye part unprotonated. In acidic medium, **1** prefers the ammonium form, which is the form protonated on the dimethylamino group in the methyl red moiety, while **2** adopts the azonium form, which is the form protonated on the azo group. Their  $pK_a$ 's are estimated to be 1.25 for **1** and 2.08 for **2**. Upon addition of guest species, **1** and **2** in acidic media near their  $pK_a$  values (pH, 1.60 for **1**; 2.52 for **2**) changed the locations of the dye parts from inside to outside the cavities, forming 1:1 inclusion complexes with the guests. The guest-induced conformation changes of **1** and **2** caused the color changes from yellow to red for **1** and from orange to red for **2**, which occur associated with the conversion of the dye parts of **1** and **2** from the azo form to the azonium one. The guest-binding properties, however, were markedly affected by structural difference of **1** and **2**, as shown by the fact that the binding constants of **2** are larger than those of **1** in acidic media and **1** loses the binding ability in neutral medium, where **2** still has binding ability. The guest selectivity of **2** observed in acidic media is remarkable for the adamantane derivatives. These results demonstrated that various color changeable indicators for molecules may be constructed on the basis of the appropriate structural design of the dye part in chromophore-modified cyclodextrins.

## Introduction

Noncovalent interactions play key roles in specific recognition of substrates by enzymes, precise replication of DNA, and folding of proteins into intricate three-dimensional forms. All biological structures and processes depend on the interplay of noncovalent interactions as well as covalent ones. In order to gain insight into the mechanisms which enable such molecular machinery to work, several model systems, whose goals include development of artificial enzymes and understanding of complexation phenomena, have been studied.<sup>1</sup> Although small synthetic organic hosts bear little resemblance to natural receptors such as enzymes and antibodies, they have more manageable degrees of structural complexity. Furthermore, they have advantages that make it possible to prepare and design the hosts so as to make them sophisticated with different functional group orientations, various degrees of flexibility, and appropriate electronic properties.

In recent years cyclodextrins (CDs) have been shown to be interesting microvessels for various molecules,<sup>2</sup> and the resulting supramolecules serve as excellent miniature models for enzyme-substrate complexes.<sup>3</sup> There are some factors in the driving force for the complexation, and hydrophobic interaction between the CD wall and the guest is certainly a primary force in aqueous solution. Due to this hydrophobic interaction and restricted free space for the guest in the CD cavity, some photophysical properties of included chromophoric guest can be affected remarkably.<sup>4</sup>

Our interest in this area has been molecular recognition of chromophore-modified cyclodextrins, with which guest species can be detected by spectroscopic changes.<sup>5</sup> The hosts usually form intramolecular complexes by including the attached chromophore moiety into their own hydrophobic cavities. Upon guest addition, the intramolecular complexes are converted into the host-guest binary complexes with releasing of the chromophore

moiety outside of the cavity. The change in the environment around the chromophore moiety from the hydrophobic interior of the cavity to bulk water solution induces remarkable changes in fluorescence and circular dichroism spectra. In the previous paper,<sup>6</sup> we have described a new host (**1**) as a guest-responsive color change indicator. This host inspired the research for detection of neutral organic species in solution. In the present study, we prepared **2** to gain insight into the mechanism of color change upon guest binding as well as to elucidate the role of the modified moiety in guest binding by comparing with **1**. The guest binding and the inclusion phenomena of the host will be shown to be greatly affected by the geometry of the dye part and the pH value of the solution.

## Results and Discussion

**pH-Dependence in Absorption Spectra of **1** and **2**.** Methyl red (**3**), which is a well-known pH indicator, undergoes a pronounced color change from yellow to red when the solution becomes acidic. Figure 1 shows the absorption spectra of **3** at various pH values. The absorption intensity around 500 nm increases, while that around 400 nm decreases with decreasing pH of the solution. When 4-(dimethylamino)azobenzene derivatives, such as methyl orange and **3**, are protonated, they take either the azonium or ammonium form, which exist in equilibrium as tautomers. The azonium form is generated by the protonation of the azo group, while the ammonium form is generated by the protonation of the dimethylamino group. The neutral azo, azonium, and ammonium forms show absorption bands around 390–460, 510–550, and 280–340 nm, respectively.<sup>7</sup> The strong peak observed around 525 nm at pH 4.0 indicates that **3** exists predominantly as the azonium form rather than as the ammonium one. *p*-Methyl red (**4**), which is the structural isomer of **3**, also exhibits the color change like **3** in the presence of acid. **4** shows the absorption maximum at 465 nm in a solution of pH 6.88 and displays a

\* Abstract published in *Advance ACS Abstracts*, June 1, 1994.

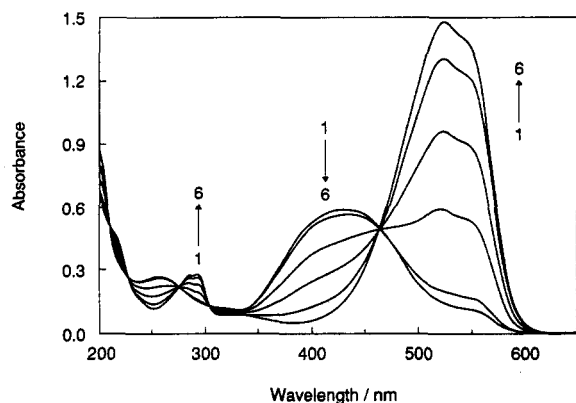
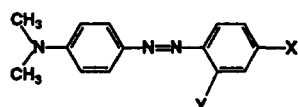
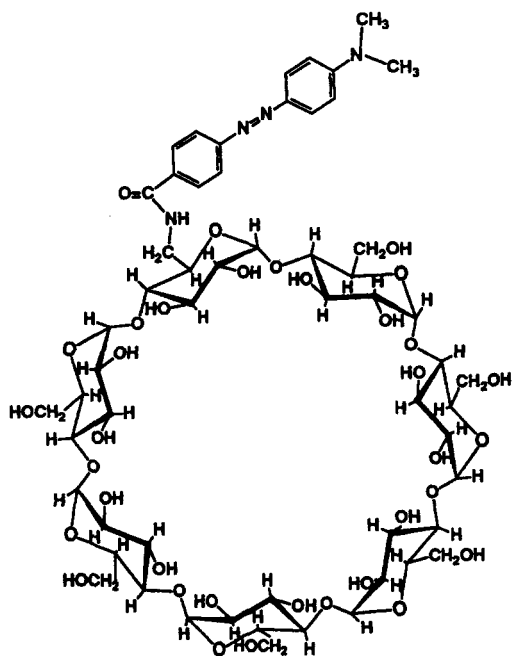


**Figure 1.** Absorption spectra of **3** ( $3.0 \times 10^{-5}$  M) in a 10% ethylene glycol aqueous solution at various pH values: (1) 6.23, (2) 5.91, (3) 5.28, (4) 4.86, (5) 4.29, (6) 3.45.



	X	Y
1	H	CONH- $\beta$ -CD
2	CONH- $\beta$ -CD	H
3	H	COOH
4	COOH	H



**2**

spectral change, decreasing and increasing in absorption intensities around 430 and 510 nm, respectively, with a progressive decrease of the pH value. Thus, it was found that **3** and **4** exist predominantly as the azonium form in acidic medium.

The absorption spectra of **1** measured at various pH values are shown in Figure 2. The isosbestic points observed at 285, 360, and 516 nm indicate that **1** exists either as unprotonated or

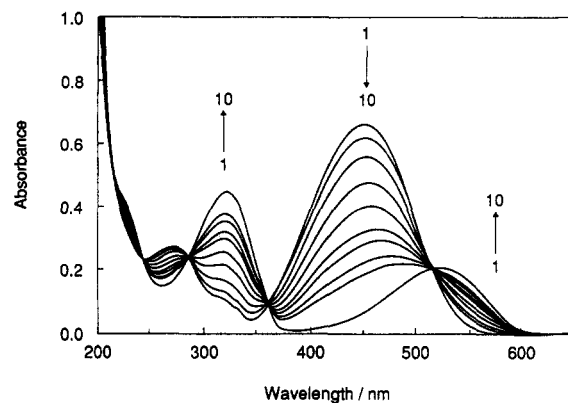


**Figure 2.** Absorption spectra of **1** ( $3.0 \times 10^{-5}$  M) in a 10% ethylene glycol aqueous solution at various pH values: (1) 6.80, (2) 2.43, (3) 1.99, (4) 1.65, (5) 1.43, (6) 1.23, (7) 1.13, (8) 1.00, (9) 0.87, (10) 1 N HCl.

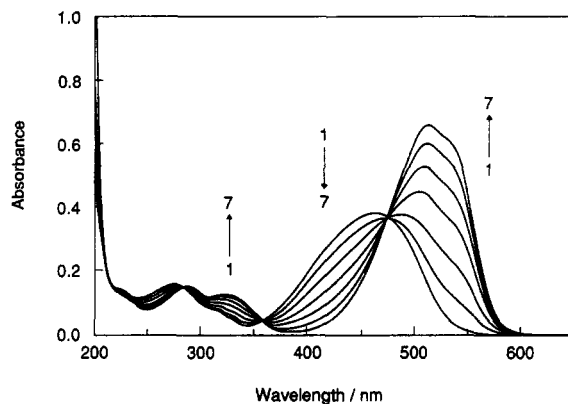


**Figure 3.** Absorption spectra of **2** ( $1.5 \times 10^{-5}$  M) in a 10% ethylene glycol aqueous solution at various pH values: (1) 6.88, (2) 2.89, (3) 2.42, (4) 2.07, (5) 1.81, (6) 1.49, (7) 0.85.

protonated species in tautomeric equilibrium. No absorption change was observed in the pH range from 6.80 to 4.0 with a maximum at 450 nm, demonstrating that the methyl red moiety of **1** is not converted into the azonium form even at pH 4.0. A further decrease in pH reduced the absorbance around 450 nm and increased the absorbances around 550 and 320 nm, these being attributed to the azonium and the ammonium forms, respectively. This observation can be explained by the inclusion of the methyl red moiety in the hydrophobic  $\beta$ -CD cavity, which protects protonation of the azo group of **1** from the acidic environment of the solution at least above pH 4.0. It is noted that the spectral shape of **1** is hardly influenced by the concentration in the range from  $3 \times 10^{-7}$  to  $6 \times 10^{-5}$  M, indicating that the inclusion of the methyl red moiety in the CD cavity occurs not intermolecularly but intramolecularly. In the intramolecular self-complexation form, the azo group of the methyl red moiety of **1** is included in its hydrophobic CD cavity, while the dimethylamino group is squeezed out from the interior of the cavity into the bulk solution at the secondary hydroxyl side of its CD. Consequently, the azo group in **1** is protected from protonation by the surrounding CD wall, while the dimethylamino group is easily protonated. Stezjli et al. found a similar absorption behavior in the methyl orange- $\beta$ -CD binary system.<sup>8</sup> They also found that inclusion complex formation of methyl orange with CD leads to a decrease in the  $pK_a$  of methyl orange. The  $pK_a$  estimated here for **1** is 1.25, while that for **3** is 4.94. This tremendous lowering of the  $pK_a$  value of **1** may be related to tight binding of the methyl red moiety in the CD cavity in the intramolecular complex. This result demonstrates that the azo group of **1** located in the hydrophobic environment in the CD cavity is hardly affected by the charge effect as it is in bulk water.

The azo group in **2** is easily protonated in acidic medium. Figure 3 shows the absorption spectra of **2** when measured at various pH

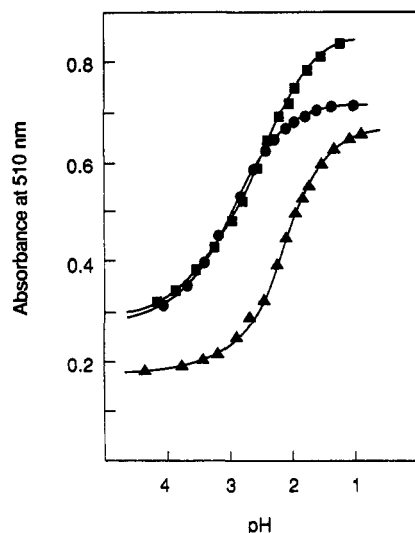


Figure 4. pH-dependence of the absorption intensity at 510 nm of **2** ( $\Delta$ ), **4** ( $\blacksquare$ ) ( $1.5 \times 10^{-5}$  M) alone, and **2** in the presence of 1-adamantanol ( $4.5 \times 10^{-4}$  M) ( $\bullet$ ).

values. This spectral variation was similar to that of **4**. The appearance of the isosbestic points at 285, 360, and 476 nm indicates that there is an equilibrium between unprotonated and protonated species. The strong peak around 510 nm observed at pH 1.0 demonstrates that **2** exists predominantly as the azonium form at this pH. The azo group in **2** is easily protonated in acidic medium. It suggests that the azo group in **2** is exposed to bulk water. However, a small decrease in the  $pK_a$  for **2** ( $pK_a = 2.08$ ) was observed as compared with that for **4** ( $pK_a = 2.58$ ) from the plots of the absorption intensities at 510 nm for **2** and **4** as a function of pH (Figure 4). This result indicates that the protonation of the azo group of the *p*-methyl red moiety in **2** is slightly suppressed due to the shallow inclusion of the *p*-methyl red moiety in the CD cavity. It is noted that the spectral shape of **2** was not affected by its concentration, confirming that this inclusion is also not intermolecular but intramolecular.

**Induced Circular Dichroism Spectra of 1 and 2.** In order to confirm the structural features of **1** and **2**, the induced circular dichroism spectra of **1** and **2** were measured. The major electronic transitions **1** and **2** are essentially those of the methyl red and the *p*-methyl red moieties themselves. From the second derivative of the absorption spectrum<sup>9</sup> of **1** at pH 6.80 in the visible region, it was found that the absorption band of **1** at 450 nm consists of two transitions with peaks at 425 and 470 nm, each ascribing to the  $\pi-\pi^*$  and the  $n-\pi^*$  transition, respectively.<sup>10</sup> Similarly, the absorption band of **2** observed at 465 nm at pH 6.88 consists of two electronic transitions with peaks at 435 and 480 nm, each ascribing to the  $\pi-\pi^*$  and the  $n-\pi^*$  transition, respectively. The transition moment of the  $\pi-\pi^*$  band (425 nm for **1** and 435 nm for **2**) of the methyl red moiety is parallel to the long axis of the dye part, while the  $n-\pi^*$  transition moment (470 nm for **1** and 480 nm for **2**) is perpendicular to the axis. Since CDs consist of chiral D-glucose, the methyl red chromophore of **1** and the *p*-methyl red one of **2** may produce induced circular dichroism in the wavelength region of the electronic transitions.<sup>11</sup>

Figure 5 and 6 show the induced circular dichroism spectra of **1** and **2** measured at various pH values, respectively. The circular dichroism sign of **1** at pH 6.80 was positive in the  $\pi-\pi^*$  transition region and negative in the  $n-\pi^*$  transition one (Figure 5). This can be interpreted in terms of axial inclusion of the methyl red moiety into its own  $\beta$ -CD cavity. With a lowering of the pH below 1.60, the intensity of the positive dichroism band around 425 nm was reduced and a new positive broad band appeared in the absorption region of the azonium form around 510 nm. These results are in agreement with the pH-induced variations observed in the absorption spectra of **1**.

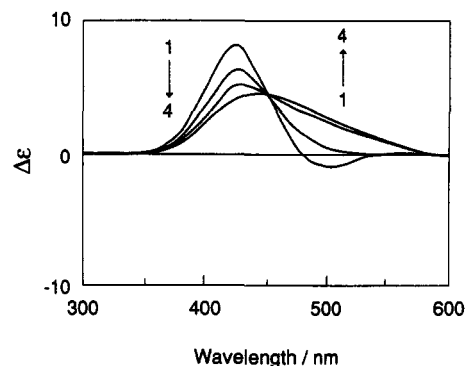


Figure 5. Induced circular dichroism spectra of **1** ( $3.0 \times 10^{-5}$  M) in a 10% ethylene glycol aqueous solution at various pH values: (1) 6.70, (2) 1.60, (3) 1.00, (4) 0.80.

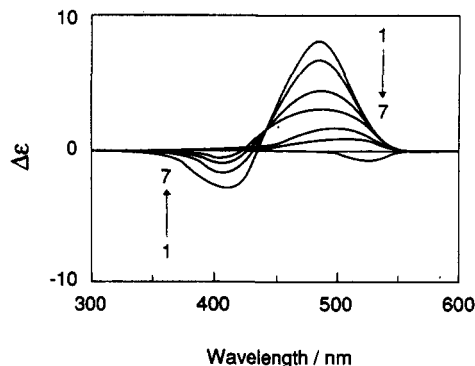
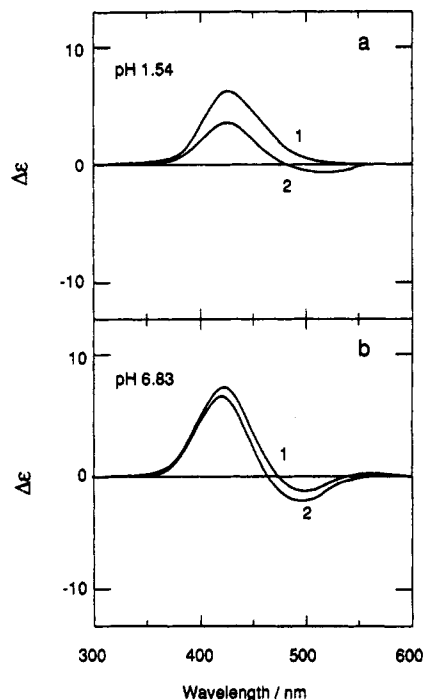


Figure 6. Induced circular dichroism spectra of **2** ( $1.5 \times 10^{-5}$  M) in a 10% ethylene glycol aqueous solution at various pH values: (1) 6.85, (2) 2.62, (3) 2.21, (4) 2.01, (5) 1.79, (6) 1.45, (7) 1.01.

The circular dichroism signs of **2** were negative for the  $\pi-\pi^*$  transition region and positive for the  $n-\pi^*$  one (Figure 6). These cotton effect signs of **2** are opposite to those of **1**. This finding can be interpreted in terms of the equatorial inclusion of the *p*-methyl red moiety into its own  $\beta$ -CD cavity; but the equatorial inclusion of such a long residue in the CD cavity seems unlikely. Perhaps the *p*-methyl red moiety of **2** lies on the surface of the primary hydroxyl group side perpendicularly to the CD axis, inserting the *p*-methyl red moiety partly into its CD cavity and consequently having a strong interaction with its hydrophobic CD cavity. The positive band around 480 nm and the negative one around 420 nm were reduced with decreasing pH. This result indicates that the interaction of the *p*-methyl red moiety with the hydrophobic CD cavity is reduced with decreasing pH because of the decrease in hydrophobicity in the *p*-methyl red moiety due to the protonation. The isoelectricity point was observed in the pH region above the  $pK_a$ , demonstrating that there exists an equilibrium between unprotonated and protonated species. In the pH region below the  $pK_a$ , however, no isoelectricity point was observed, suggesting that a system composed of more than two species is involved.

**Guest-Induced Structural Variations of 1 and 2.** In the previous paper,<sup>6</sup> we have demonstrated that **1** formed inclusion complexes with some guests at pH 1.60, accompanied by a color change from yellow to red. The absorption maximum of **1** was at 455 nm at pH 1.60 in the absence of a guest, suggesting that the methyl red moiety of **1** exists as the azo form. Upon the addition of 1-adamantanol as a guest, the absorption intensity around 510 nm increased, while that around 450 nm decreased. This spectral change was explained by the exclusion of the methyl red moiety from inside to outside the CD cavity. The environment change around the methyl red moiety from the hydrophobic medium in the CD cavity to the bulk water resulted in the protonation of the azo group in the methyl red moiety to form the azonium form, causing the color change. The appearance of isosbestic points at



**Figure 7.** Induced circular dichroism spectra of **1** ( $3.0 \times 10^{-5}$  M) in a 10% ethylene glycol aqueous solution, alone or in the presence of 1-adamantanol: (a) pH 1.54; 1-adamantanol concentrations, (1) 0, (2)  $9.0 \times 10^{-4}$  M; (b) pH 6.83; 1-adamantanol concentration, (1) 0, (2)  $1.2 \times 10^{-3}$  M.

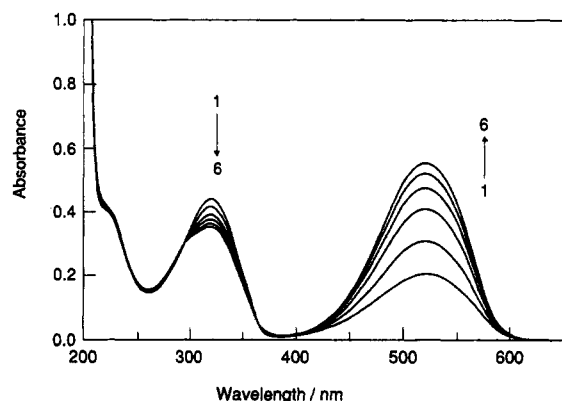


**Figure 8.** Absorption spectra of **1** ( $3.0 \times 10^{-5}$  M) in a 1 N HCl-10% ethylene glycol aqueous solution with various concentrations of 1-adamantanol: (1) 0, (2)  $1.2 \times 10^{-4}$ , (3)  $3.0 \times 10^{-4}$ , (4)  $4.8 \times 10^{-4}$ , (5)  $6.6 \times 10^{-4}$ , (6)  $8.4 \times 10^{-4}$  M.

278, 356, and 470 nm for the solution at different guest concentrations of 1-adamantanol indicates that **1** forms a 1:1 inclusion complex.

This structural change of **1** was confirmed from the induced circular dichroism spectra of **1** (Figure 7a). It was observed that the positive band around 420 nm decreased and a negative one around 510 nm, which is the absorption region of the azonium form, appeared upon the addition of 1-adamantanol. This indicates that the methyl red moiety included in its CD cavity as the azo form is excluded to the outside of the cavity by 1-adamantanol so as to be oriented perpendicular to the CD axis as the azonium form. This spectral change became more remarkable with increasing concentrations of 1-adamantanol.

In 1 N HCl-10% ethylene glycol aqueous solution, we observed the hyperchromic effect of **1** in absorption spectra upon guest addition, as shown in Figure 8. The absorption bands around 320 and 520 nm were observed in the absence of the guest, indicating that **1** exists either in the ammonium or the azonium form in a tautomeric equilibrium. Upon the addition of 1-adamantanol, the band around 320 nm decreased and that

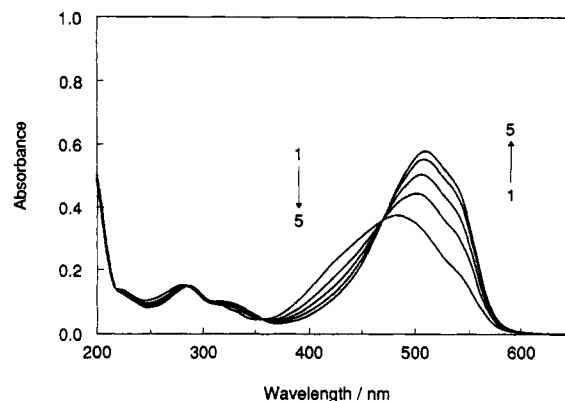


**Figure 9.** Absorption spectra of **2** ( $1.5 \times 10^{-5}$  M) in a 10% ethylene glycol aqueous solution with various concentrations of 1-adamantanol at pH 2.52: (1) 0, (2)  $3.0 \times 10^{-5}$ , (3)  $6.0 \times 10^{-5}$ , (4)  $1.2 \times 10^{-4}$ , (5)  $3.0 \times 10^{-4}$  M.

around 520 nm increased remarkably. This spectral change indicates that the ammonium form of **1** is converted into the azonium form upon 1-adamantanol addition. This can also be explained by the exclusion of the methyl red moiety from inside to outside the CD cavity, as in the case of pH 1.60. The degree of guest-induced change in absorption spectra, however, was more sensitive than the case of pH 1.60, suggesting that the methyl red moiety of **1** is easily excluded in lower pH conditions due to a decrease of hydrophobicity in the methyl red moiety by protonation.

In neutral medium at pH 6.83, the absorption peak at 450 nm of **1** was slightly red shifted upon the addition of an excess of 1-adamantanol. The effects of the guest addition on the circular dichroism spectrum were also small, as shown by small degrees of decrease and increase in the absolute intensity for the positive and the negative band around 420 and 480 nm, respectively (Figure 7b). Similar spectral behavior of **1** was obtained even at pH 4.0, where **3** exists predominantly as the azonium form. These small spectral changes suggest that it is hard for **1** to form the inclusion complex with the guest even in a weakly acidic medium as well as in a neutral one. In other words, the methyl red moiety of **1** is too tightly included in its cavity to accommodate the guest. Therefore, the methyl red moiety in **1** acts as an inhibitor for guest binding under these conditions.

These results indicate that the guest-binding ability of **1** is affected by pH remarkably. This behavior of **1** may be related to the change in the degree of hydrophobicity of the methyl red moiety, more hydrophobic in the neutral medium than in the acidic milieu.

When 1-adamantanol was added to the acidic solution of **2**, absorption spectral changes were observed similar to the case of **1**, accompanied by the color change from orange to red. However, these spectral changes were small as compared with those for **1**. Figure 9 shows the absorption spectra of **2**, alone and in the presence of 1-adamantanol at pH 2.52. The predominant absorption maximum around 485 nm of **2** indicates that the azo form is the dominant species rather than the azonium one at this pH. The addition of 1-adamantanol increased the absorption intensity around 510 nm, suggesting that the azo form of the *p*-methyl red moiety in **2** is converted into the azonium one. This spectral change suggests that the *p*-methyl red moiety was excluded from the cavity by 1-adamantanol to form an inclusion complex. The fact that there are isosbestic points at 358 and 470 nm confirms that the stoichiometry of the complex formation is 1:1.

Figure 10a shows the induced circular dichroism spectra of **2** in the absence and the presence of 1-adamantanol at pH 2.52. Upon the addition of 1-adamantanol, the positive dichroism band around 480 nm disappeared and the negative one appeared around 510 nm. This indicates that the *p*-methyl red moiety, which is

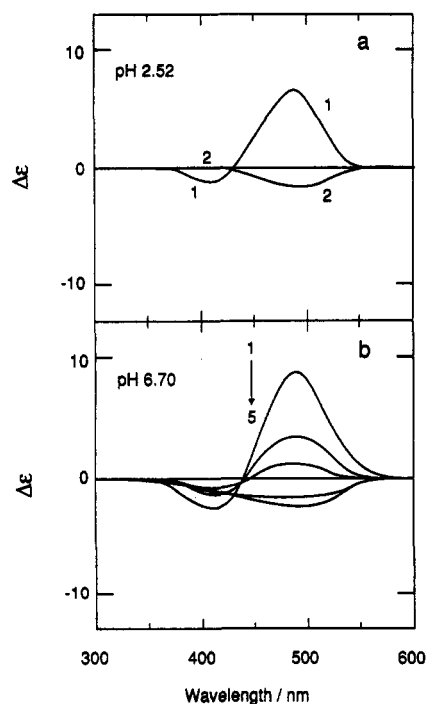


**Figure 10.** Induced circular dichroism spectra of **2** ( $1.5 \times 10^{-5}$  M) in a 10% ethylene glycol aqueous solution, alone or in the presence of 1-adamantanol: (a) pH 2.52; 1-adamantanol concentration, (1) 0, (2)  $4.2 \times 10^{-4}$  M; (b) pH 6.70; 1-adamantanol concentration, (1) 0, (2)  $7.5 \times 10^{-5}$ , (3)  $1.5 \times 10^{-4}$ , (4)  $3.0 \times 10^{-4}$ , (5)  $6.0 \times 10^{-4}$  M.

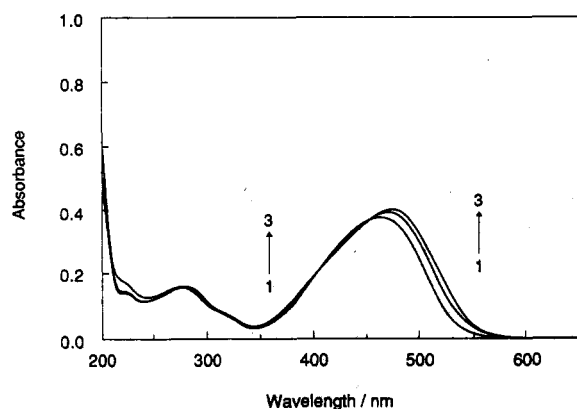


**Figure 11.** Absorption spectra of **2** ( $1.5 \times 10^{-5}$  M) in a 10% ethylene glycol aqueous solution with various concentrations of 1-adamantanol at pH 6.80: (1) 0, (2)  $7.5 \times 10^{-5}$ , (3)  $4.5 \times 10^{-4}$  M.

included in the CD cavity as the azo form with an orientation nearly perpendicular to the CD axis (equatorial inclusion), is excluded from the cavity by 1-adamantanol, resulting in the conversion into the azonium form. Although this behavior of **2** was basically similar to that of **1**, it should be emphasized that the inclusion of the *p*-methyl red moiety must be shallow because of its equatorial orientation in the CD cavity.

Figure 11 shows the absorption spectra of **2** in neutral medium at pH 6.80 containing various concentrations of 1-adamantanol. The absorption maximum of **2** observed at 465 nm in the absence of 1-adamantanol is red shifted with increasing concentrations of 1-adamantanol. The conformation change of **2** occurring associated with the formation of an inclusion complex may be reflected in the shift. It is considered that the CD cavity of **2** has a space to include the guest because of the shallow inclusion of the *p*-methyl red moiety. The isosbestic point at 460 nm indicates the formation of a 1:1 inclusion complex of **2** with 1-adamantanol.

This conformation change of **2** was confirmed from the induced circular dichroism of **2** (Figure 10b). The intensity of the positive dichroism band around 480 nm in the absorption region of the

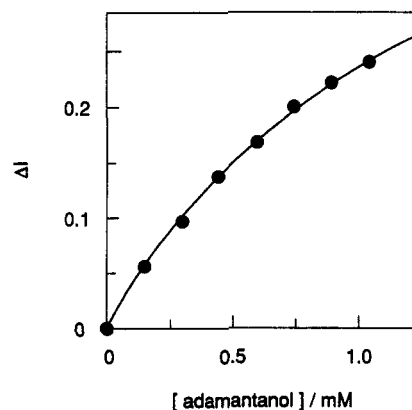


**Figure 12.** Curve-fitting data for the absorption intensities of **1** at 510 nm at different concentrations of 1-adamantanol at pH 1.60.

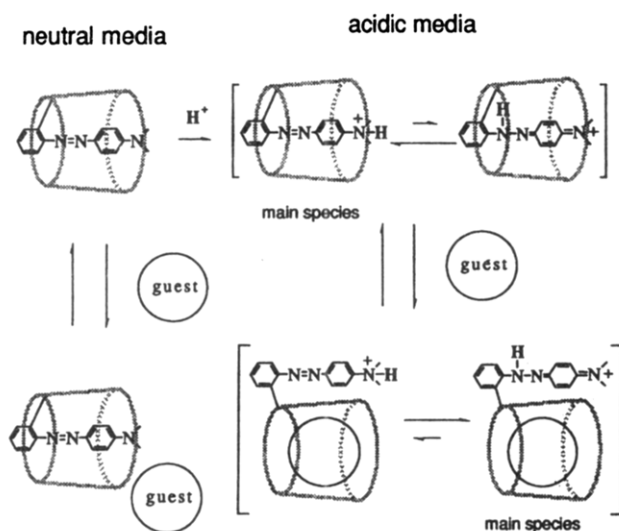
**TABLE 1: Binding Constants of 1 with Adamantane Derivatives**

guest	$K$ ( $M^{-1}$ )	
	pH 1.60	1 N HCl
1-adamantanecarboxylic acid	5550	15 800
1-adamantanol	730	1980

*p*-methyl red moiety decreased markedly with increasing concentrations of 1-adamantanol, and the broad negative band appeared at high concentrations of 1-adamantanol. This result may be explained in terms of the exclusion of the *p*-methyl red moiety from the CD cavity associated with the complexation of **2** with 1-adamantanol. Furthermore, as seen in Figure 4, the absorption intensity at 510 nm of **2** in the presence of 1-adamantanol plotted as a function of pH is similar to that of **4**, suggesting that the environment around the *p*-methyl red moiety excluded from the cavity by the guest is similar to that around **4**. So we can conclude that the *p*-methyl red moiety of **2** in the presence of the guest has almost no interaction with its CD cavity and is totally exposed to the bulk water. When the concentration of 1-adamantanol is low, there exists an isosbestic point, indicating that 1:1 stoichiometry for the complexation. At high concentrations of 1-adamantanol, other species may be involved in the system.

**Binding Constants for 1 and 2.** The spectral changes of **1** and **2** induced by formation of the inclusion complexes may be used for determining the binding constants. Figure 12 shows the guest-induced change in absorbance at 510 nm for **1** as a function of guest concentration. A typical saturation curve for **1** and 1-adamantanol was obtained by a nonlinear least squares fitting procedure. The same curve-fitting analysis could be applied to other guests with good fitting. Table 1 shows the binding constants of **1** for 1-adamantanecarboxylic acid and 1-adamantanol; both are good guests for **1** in a solution of pH 1.60 and 1 N HCl.<sup>12</sup> As shown in Scheme 1, **1** has no binding ability in the weakly acidic medium as well as in the neutral one because of the tight inclusion of the methyl red moiety. The methyl red moiety in **1** acts as an intramolecular inhibitor for guest binding under these conditions. In acidic medium, this tight inclusion is loosened by protonation on the methyl red moiety, resulting in the formation of inclusion complexes with various guests. The binding constants of **1** at pH 1.60, however, are small as compared with the native CD.<sup>13</sup> This demonstrates that the methyl red moiety at pH 1.60 still acts as an intramolecular weak inhibitor for guest binding. In 1 N HCl aqueous solution, however, **1** has binding abilities similar to those of  $\beta$ -CD. Since ca. 95% of **1** is protonated on the methyl red moiety under this condition, the methyl red moiety in **1** does not act as the inhibitor for guest binding. At pH 1.60, ca. 70% of **1** is unprotonated, and the unprotonated species does not contribute appreciably to the guest binding, resulting in binding constants of ca. 35% of those in 1 N HCl aqueous solution. So

## SCHEME 1



## SCHEME 2

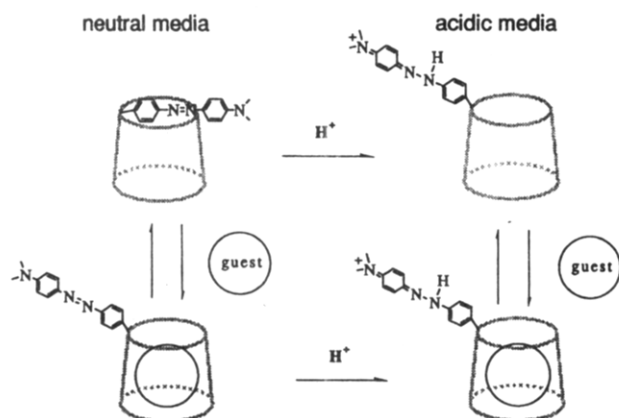


TABLE 2: Binding Constants of 2 with Various Guests

guest	K (M <sup>-1</sup> )	
	pH 2.52	pH 7.20
1-adamantanecarboxylic acid	264 000	6210
1-adamantanol	35 200	7200
borneol	15 200	3780
cyclooctanol	2570	430
cyclohexanol	250	150

we can conclude that the binding constant of **1** for each guest is governed by the ratio of the protonated species of **1**.

The binding constants of **2** at pH 2.52 and 7.20 were also estimated in the same manner as the case of **1**, as shown in Table 2. Because of the shallow inclusion of the *p*-methyl red moiety in its CD cavity, the cavity of **2** has a space where a guest molecule can be included, as shown in Scheme 2. Although the interaction between the *p*-methyl red moiety and the CD cavity exists, the protonation on the *p*-methyl red moiety can easily decrease this interaction. The guest binding of **2** in acidic medium also decreased the interaction between the *p*-methyl red moiety and the CD cavity, promoting the protonation on the *p*-methyl red moiety. The binding constants for **2** with the guests in acidic medium are much larger than those in neutral medium as in the case of **1**. These observations can be explained in terms of the degree of interaction of the *p*-methyl red moiety with the CD cavity. The strong interaction of the *p*-methyl red moiety with CD cavity in neutral medium makes the moiety difficult to be replaced by the guests. The situation for **2** is the same as that for **1**, but the inhibitory effect of **2** is much smaller than that of **1** because of shallow binding of the *p*-methyl red moiety to the CD cavity.

The order of the binding constants of **2** at pH 2.52 is the same as that of the binding constants of **1** at pH 1.60, being ca. 50-fold larger than those of **1** for 1-adamantanecarboxylic acid and 1-adamantanol. The structural difference between **1** and **2** may be reflected in the difference of the binding constants. The binding constants of **2** in acidic medium is ca. 5-fold larger than those in neutral medium except for 1-adamantanecarboxylic acid. The binding constant of **2** for 1-adamantanol is larger than that for 1-adamantanecarboxylic acid in neutral medium, whereas the binding constant of **2** for 1-adamantanecarboxylic acid is ca. 40-fold larger in acidic medium than that in a neutral one. This can be explained by the fact that the negative charge of 1-adamantanecarboxylic acid suppresses the inclusion of this guest in the hydrophobic CD cavity in neutral conditions.

## Conclusion

The chromophore-modified CDs, **1** and **2**, both bearing the 4-(dimethylamino)azobenzene residue, have different orientations, parallel and perpendicular to the CD axis for **1** and **2**, respectively. As a result, the dye part of **1** is accommodated in the  $\beta$ -CD cavity, while that of **2** is not fully included in the cavity, probably being shallowly inserted into the cavity. The structural difference between **1** and **2** resides only in the position of the amide bond which links the 4-(dimethylamino)azobenzene residue to the  $\beta$ -CD unit, *ortho* and *para* with respect to the azo group, respectively. However, the binding abilities and guest-responsive features were markedly different between the hosts. These results demonstrate that guest binding and spectroscopic properties of chromophore-modified CDs can be remarkably modulated by varying the chromophore structures. Many color change indicators for detecting various organic compounds will be constructed on this basis.

## Measurements

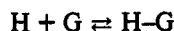
Absorption spectra were recorded on a Shimadzu UV-3100 spectrophotometer. Induced circular dichroism spectra were measured with a JASCO J-600 spectropolarimeter. All spectroscopic measurements were made at 25 °C in a 10% ethylene glycol aqueous solution except for **4**, where a 50% ethylene glycol aqueous solution was used because of poor solubility. The concentration of the solution for **1** and **3** was 0.03 mM, while that for **2** and **4** was 0.015 mM because of poor solubility. <sup>1</sup>H-NMR spectra were run on a Varian VXR-500 spectrometer in DMSO-*d*<sub>6</sub>. The pH of the solution was measured on a TOA pH meter HM-60S, which had been calibrated at 25 °C with pH standard solutions of pH 4.01 ± 0.01 and 6.86 ± 0.01. Hydrochloric acid was used to set the pH in the acidic region, and formate buffer was used in the case of guest addition at pH 4.0. Phosphate buffer was used in the measurements for binding constants of **2** to set the pH at 7.20.

The  $pK_a$  of **1–4** was estimated by the following equation.

$$\Delta I = \frac{K_a \Delta I_{\max} \times 10^{-pH}}{1 + K_a \times 10^{-pH}}$$

where  $K_a$  is the acid–base dissociation constant of the unprotonated and protonated forms of **1–4**, which exist as in the tautomeric equilibrium of azo or dimethylamino groups. Under neutral conditions, it is assumed that **1–4** exist almost totally as the azo form. The absorption intensities at 450 nm for **1** and at 510 nm for **2–4** are abbreviated as  $I_0$  under neutral conditions and those at a certain pH as  $I$ , and  $\Delta I$  is  $I_0 - I$ . When **1–4** are totally converted into protonated forms,  $\Delta I$  is equal to  $\Delta I_{\max}$ . The uncertainties in  $pK_a$  were always less than ±0.03 logarithmic unit.

In this system, the following equation describes the complexation equilibrium.



where H, G, and H-G represent free host, free guest, and host-guest complex, respectively. The binding constants of 1 and 2 for several guests, K, were defined by the following equation.

$$K = \frac{C}{(H_0 - C)(G_0 - C)} \quad (1)$$

where  $H_0$ ,  $G_0$ , and C represent the initial concentrations of host, guest, and the complex, respectively. The difference in the absorption intensity at 510 nm between the host and the host in the presence of guest is expressed as the  $\Delta I$  value. The concentration of the complex, C, is reflected in the magnitude of  $\Delta I$ . When the hosts exist totally as the inclusion complexes,  $\Delta I$  is equal to  $\Delta I_{\max}$ . Using the values of  $H_0$ ,  $G_0$ ,  $\Delta I$ , and  $\Delta I_{\max}$ , eq 1 may lead to the following representation.

$$K = \frac{\Delta I / \Delta I_{\max}}{(1 - \Delta I / \Delta I_{\max})(G_0 - \Delta I \times H_0 / \Delta I_{\max})} \quad (2)$$

Therefore,

$$\Delta I = \frac{\Delta I_{\max} [(G_0 + H_0 + 1/K) - \{(G_0 + H_0 + 1/K)^2 - 4G_0H_0\}^{1/2}]}{2H_0} \quad (3)$$

The binding constant of each host with a guest, K, is estimated by fitting eq 3 to the data obtained.

## Materials

$\beta$ -CD was a kind gift from Nihon Shokuhin Kako Co. Ltd. Compounds 3 and 4 and all reagents as guests were purchased from Tokyo Kasei and were used without further purification. Ethylene glycol used for spectroscopic measurements was spectral grade.

## Synthesis

**6-Deoxy-6-amino[2-[4-(dimethylamino)phenylazo]benzoyl]- $\beta$ -cyclodextrin (1).** A solution of 3 (1.75 g, 6.61 mmol) and dicyclohexylcarbodiimide (DCC) 1.50 g, 7.28 mmol in dimethylacetamide (DMAc) was stirred at 0 °C for 10 min. To the mixture was added 6-deoxy-6-amino- $\beta$ -cyclodextrin (3.0 g, 2.65 mmol), and the resultant solution was stirred at 0 °C for 5 h and then at room temperature for 10 h. After DMAc was removed by evaporation under reduced pressure, the reaction mixture was poured into acetone (500 mL) to form precipitates. The precipitates were collected by filtration and then washed with acetone (300 mL) several times. They were poured into 1 L of hot water to remove insoluble materials by filtration. After cooling, the solid crude products were obtained by filtration. Recrystallization from the mixture of methanol and water (9:1 v/v) gave the product as orange powder (290 mg, 7.4%):  $R_f$  0.44 (n-butanol-ethanol-water 5:4:3);  $^1\text{H-NMR}$  (DMSO- $d_6$ ; 500 MHz)  $\delta$  3.22 (6H, s), 3.28–4.00 (m), 4.51–4.76 (6H, m), 4.88–

5.00 (7H, m), 5.75–5.95 (14H, m), 7.00 (2H, d), 7.61 (1H, t), 7.69 (1H, t), 7.83 (1H, d), 7.94 (2H, d), 8.11 (1H, d), 9.11 (1H, t). Anal. Calcd for  $\text{C}_{57}\text{H}_{84}\text{N}_4\text{O}_{35} \cdot 5\text{H}_2\text{O}$ : C, 46.40; H, 6.42; N, 3.80. Found: C, 46.21; H, 6.58; N, 3.84.

**6-Deoxy-6-amino[4-[4-(dimethylamino)phenylazo]benzoyl]- $\beta$ -cyclodextrin (2).** A solution of 4 (1.75 g, 6.61 mmol), DCC (1.50 g, 7.28 mmol), and 1-hydroxybenzotriazole (HOBt) (1.0 g, 7.40 mmol) in DMAc was stirred at 0 °C for 10 min. To the mixture was added 6-deoxy-6-amino- $\beta$ -cyclodextrin (3.0 g, 2.65 mmol), and the resultant solution was stirred at 0 °C for 5 h and then at room temperature for 10 h. The product was purified in the same manner as in the case of 1 and was obtained as orange powder (240 mg, 6.1%):  $R_f$  0.46 (n-butanol-ethanol-water 5:4:3);  $^1\text{H-NMR}$  (DMSO- $d_6$ ; 500 MHz)  $\delta$  3.06 (6H, s), 3.10–3.72 (m), 3.82–3.96 (2H, m), 4.34–4.50 (6H, m), 4.74–4.96 (7H, m), 5.55–5.90 (14H, m), 6.82 (2H, d), 7.77 (2H, d), 7.82 (2H, d), 7.95 (2H, d), 8.36 (1H, t). Anal. Calcd for  $\text{C}_{57}\text{H}_{84}\text{N}_4\text{O}_{35} \cdot 6\text{H}_2\text{O}$ : C, 45.84; H, 6.48; N, 3.75. Found: C, 45.95; H, 6.01; N, 3.68.

## References and Notes

- (1) (a) Rebek, J., Jr. *Science* **1987**, *235*, 1478. (b) Lehn, J. *Angew. Chem., Int. Ed. Engl.* **1988**, *27*, 89. (c) Cram, D. J. *Angew. Chem., Int. Ed. Engl.* **1988**, *27*, 1009.
- (2) Bender, M. L.; Komiyama, M. *Cyclodextrin Chemistry*; Springer-Verlag: Berlin, 1978.
- (3) (a) Breslow, R.; *Science* **1982**, *218*, 532. (b) Ramamurthy, V.; Eaton, D. F. *Acc. Chem. Res.* **1988**, *21*, 300. (c) D'Souza, V. T.; Bender, M. L. *Acc. Chem. Res.* **1987**, *20*, 146. (d) Breslow, R.; Zhang, B. *J. Am. Chem. Soc.* **1992**, *114*, 5882. (e) Moorthy, J. N.; Venkatesan, K.; Weiss, R. G. *J. Org. Chem.* **1992**, *57*, 3293.
- (4) (a) Cramer, F.; Saenger, W.; Spatz, H.-Ch. *J. Am. Chem. Soc.* **1967**, *89*, 14. (b) Nag, A.; Dutta, R.; Chattopadhyay, N.; Bhattacharyya, K. *Chem. Phys. Lett.* **1989**, *157*, 83. (c) Buvari, A.; Barcza, L. *J. Inclusive Phenom.* **1989**, *7*, 103. (d) Barcza, L.; Buvari, A. *Carbohydr. Res.* **1989**, *192*, 103.
- (5) (a) Ueno, A.; Suzuki, I.; Osa, T. *J. Am. Chem. Soc.* **1989**, *111*, 6391. (b) Ueno, A.; Moriawaki, F.; Azuma, A.; Osa, T. *Carbohydr. Res.* **1989**, *192*, 173. (c) Ueno, A.; Fukushima, M.; Osa, T. *J. Chem. Soc., Perkin. Trans. 2* **1990**, 1067. (d) Ueno, A.; Minato, S.; Suzuki, I.; Fukushima, M.; Ohkubo, M.; Osa, T.; Hamada, F.; Murai, K. *Chem. Lett.* **1990**, 605. (e) Minato, S.; Osa, T.; Morita, M.; Nakamura, A.; Ikeda, H.; Toda, F.; Ueno, A. *Photochem. Photobiol.* **1991**, *54*, 593. (f) Fukushima, M.; Osa, T.; Ueno, A. *Chem. Lett.* **1991**, 709. (g) Wang, Y.; Ikeda, T.; Ueno, A.; Toda, F. *Chem. Lett.* **1992**, 863. (h) Ueno, A.; Minato, S.; Osa, T. *Anal. Chem.* **1992**, *64*, 1154. (i) Hamasaki, K.; Ueno, A.; Toda, F. *J. Chem. Soc., Chem. Commun.* **1993**, *3*, 331.
- (6) Ueno, A.; Kuwabara, T.; Nakamura, A.; Toda, F. *Nature* **1992**, *356*, 136.
- (7) (a) Yamamoto, S.; Nishimura, N.; Hasegawa, N. *Bull. Chem. Soc. Jpn.* **1973**, *46*, 194. (b) Yamamoto, S. *Bull. Chem. Soc. Jpn.* **1973**, *46*, 3139.
- (8) Szejtli, J. *Cyclodextrins and Their Inclusion Complexes*; Akademiai Kiado: Budapest, 1982.
- (9) Giese, A. T.; French, C. S. *Appl. Spectrosc.* **1955**, *9*, 78.
- (10) Kroner, J.; Bock, H. *Chem. Ber.* **1968**, *101*, 1922.
- (11) (a) Harata, K.; Uedaira, H. *Bull. Chem. Soc. Jpn.* **1975**, *48*, 375. (b) Shimizu, H.; Kaito, A.; Hatano, M. *Bull. Chem. Soc. Jpn.* **1979**, *52*, 2678. (c) Kodaka, M.; Fukaya, T. *Bull. Chem. Soc. Jpn.* **1989**, *62*, 1154.
- (12) In the previous paper (ref 6), we employed the following equation for estimation of the binding constants.

$$\Delta I = KG\Delta I_{\max} / (1 + KG)$$

This equation is assumed to be correct in the case where  $G \gg H-G$ , where G is the concentration of the guest added.

- (13) Eftink, M. R.; Andy, M. L.; Bystrom, K.; Perlmutter, H. D.; Kristol, D. S. *J. Am. Chem. Soc.* **1989**, *111*, 6391.